

## Raman scattering in $\beta$ -alumina\*

C. H. Hao, L. L. Chase,<sup>†</sup> and G. D. Mahan

*Physics Department, Indiana University, Bloomington, Indiana 47401*

(Received 11 December 1975)

The Raman spectra of the ionic conductor Na  $\beta$ -Al<sub>2</sub>O<sub>3</sub> and several of its cation-substituted isomorphs have been studied at temperatures from 4.2 to 900 °K. For the Na, Ag, K, and Rb isomorphs, but not for Li, low-frequency vibrations are observed which are attributed to vibrations of the mobile cations with displacements parallel to the conducting planes. In several cases the frequencies and widths of these vibrations are quite different from those measured by infrared reflectivity. A calculation of the contribution of dipolar interactions to the in-phase vibrations of the cations shows that the resulting corrections are sizable, but are essentially identical for ir and Raman modes. The differences in the spectra may be due to a difference in the samples used. A quasielastic scattering wing is observed at high temperatures in Ag  $\beta$ -Al<sub>2</sub>O<sub>3</sub>. The estimated width of this feature is consistent with the ionic hopping rate calculated from the attempt frequency and activation energy for ionic conduction. Structural distortion modes of the spinel blocks are also observed. These correspond to vibrations observed by neutron scattering. Possible assignments for these modes are suggested by their polarization behavior. Two different possible superlattices in Ag  $\beta$ -alumina and in Na, K, and Rb  $\beta$ -alumina are discussed and related to the splittings in the low-frequency vibrations of the cations.

### I. INTRODUCTION

The potential use of superionic conductors in future battery systems has attracted great attention from both theorists and experimentalists in order to investigate and gain insight into the mechanisms for the high ionic conductivities of these materials. Considering only the superionic conductors  $\beta$ -alumina, one finds that experimental techniques such as Raman scattering,<sup>1</sup> NMR,<sup>2</sup> tracer diffusion,<sup>3,4</sup> far-infrared reflection spectroscopy,<sup>5</sup> x-ray diffuse scattering,<sup>6-8</sup> and neutron scattering<sup>9</sup> have all been used to collect information about the behavior of the cations in  $\beta$ -alumina. Theoretically, models based on trapped and free ion states,<sup>10</sup> diffusion in an interacting system,<sup>11</sup> collective behavior,<sup>12</sup> liquidlike description of ionic carriers in transport theory,<sup>13</sup> etc. have also been published. Here we will present the results of Raman scattering from Li<sup>+</sup>, Na<sup>+</sup>, K<sup>+</sup>, Rb<sup>+</sup>, and Ag<sup>+</sup> in  $\beta$ -alumina in the wave number range from 0 to about 850 cm<sup>-1</sup>, and in the temperature range from 4.2 to over 850 °K for some of these ions. A preliminary report has already been published.<sup>1</sup>

The structure of  $\beta$ -alumina has a unit cell consisting of spinel blocks separated by two mirror planes perpendicular to the *c* axis.<sup>14,15</sup> Each mirror plane has a hexagonal network of O<sup>2-</sup> in between which are the so-called Beavers-Ross (BR) sites, anti-Beavers-Ross sites, and the mid-oxygen sites. The cations reside in some of the above-mentioned sites and can hop from one site to the other with a rather small activation energy of ~ 0.2 eV for Na<sup>+</sup> or Ag<sup>+</sup>. This accounts for the high conductivity of this material.

The infrared data of Allen and Remeika<sup>5</sup> for Na

and Ag  $\beta$ -alumina showed absorption bands which were interpreted as the vibrational frequency for a cation in the BR site. Our early Raman work<sup>1</sup> obtained essentially the same frequencies as the infrared data, but with a much narrower line for Na  $\beta$ -alumina. These narrower lines have now been observed in other infrared work.<sup>16</sup> Thus the line widths seem dependent on the manner in which the crystals are grown. Now we wish to report similar attempt frequencies in K and Rb  $\beta$ -alumina. None is observed in Li. These results are similar to recent infrared data, which also fail to observe a mode for Li, but do for the other ions.<sup>8</sup> We report Raman data for five different cations in  $\beta$ -alumina, over a wide temperature range, and for different polarizations. Many different Raman lines are observed. Pure Al<sub>2</sub>O<sub>3</sub> has no Raman or ir modes below 385 cm<sup>-1</sup>.<sup>17,18</sup> There are many in  $\beta$ -alumina. Several of these can be associated with the motion of cations or oxygens in the mirror planes, or with gross distortions of the spinel blocks.

By way of background material, we wish to summarize recent experimental results on the cation motion in the mirror planes of  $\beta$ -alumina. The central question appears to be the nature of the nonstoichiometry. Stoichiometric Na  $\beta$ -alumina would have each Na ion in a BR site, and none in the anti-BR or midoxygen sites. Typical Na  $\beta$ -alumina has an excess of about 25% Na<sub>2</sub>O, which goes into the mirror plane.<sup>8,14,15</sup> Roth proposed a model,<sup>15</sup> based on his x-ray data, which had the two Na and one O in three adjacent midoxygen sites. This forms a stable defect structure, which does not participate in conduction. Another model proposed by Wang, Gaffari, and Choi<sup>19</sup> ignores

the O excess, and just occupies some cells in the mirror plane with two Na ions rather than one in the BR site. These two occupy midoxygen positions, and provide the center which participates in conduction. This latter model has been supported by McWhan *et al.*<sup>8,9</sup>

Another exciting experimental result is the reported superlattice at low temperature.<sup>8-8</sup> There seems to be conflicting reports whether this superlattice changes with temperature.

## II. EXPERIMENTAL METHODS

Our sample of Na  $\beta$ -alumina was obtained from Union Carbide Corp. The Ag, Li, K, and Rb isomorphs were prepared by heating the Na  $\beta$ -alumina in molten  $\text{AgNO}_3$ ,  $\text{LiCl}$ ,  $\text{KCl}$ ,  $\text{RbCl}$ , respectively, for 48 h or more.<sup>3</sup>

The data were collected in  $90^\circ$  scattering geometry using the 5145 Å Argon line, polarized in the proper plane, as source and a system of Spex double monochromator, cooled photomultiplier tube, and multichannel analyzer, and other electronics to detect and store the scattered light signals. Data were collected for different cations at various temperatures and with different incident and scattered polarizations.

## III. EXPERIMENTAL RESULTS

The structure of  $\beta$ -alumina is hexagonal, and has the space group  $P6_3/mmc$ . By considering only the mobile cations in the unit cell, one can arrive at the result that the only Raman-active mode transforms as  $E_{2g}$  in the  $D_{6h}$  point group. In this mode the cations in the two mirror planes are vibrating in the plane but are  $180^\circ$  out of phase with each other. If the oxygen ions in the mirror planes are included, the number of modes of each symmetry is simply doubled. As a result the oxygen ion motions will also contribute to the  $E_{2g}$  (XX and XY) spectrum. There are no Raman active modes for scattering from a  $\text{Na}^+$  ion vibrating in the Z direction. Of course, the selection rule applies to the ideal structure. The significant amount of nonstoichiometry may introduce disorder, which may permit breaking of selection rules. Thus the z vibrations may be weakly observable, despite the fact that they transform as the  $B_{2g}$ , silent representation of  $D_{6h}$ . The Raman-active vibrations of  $D_{6h}$  are, with allowed polarizations in parentheses:  $A_{1g}$  (XX, YY, ZZ);  $E_{1g}$  (XZ, YZ);  $E_{2g}$  (XX, YY, XY).

The Raman scattering spectra of  $\text{Li}^+$ ,  $\text{Na}^+$ ,  $\text{K}^+$ ,  $\text{Rb}^+$ , and  $\text{Ag}^+$  in  $\beta$ -alumina are shown in Figs. 1-3.

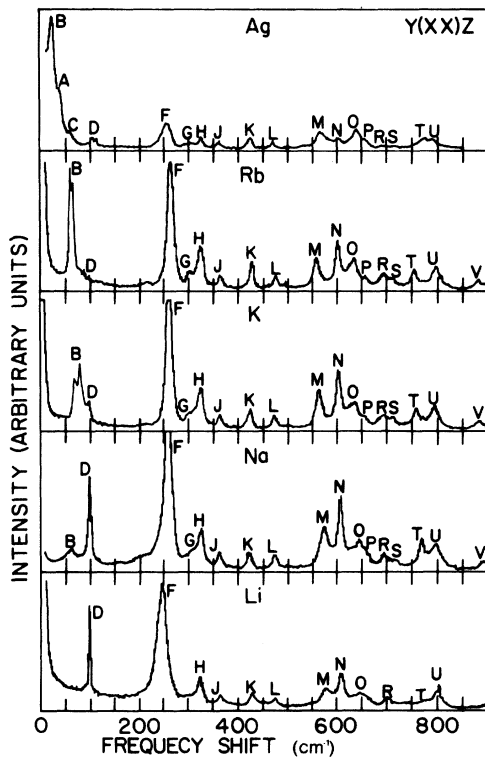


FIG. 1.  $Y(XX)Z$  spectra of  $\beta\text{-Al}_2\text{O}_3$  isomorphs obtained at  $300^\circ\text{K}$  for Rb, K, Na, and Li, and at  $77^\circ\text{K}$  for Ag.

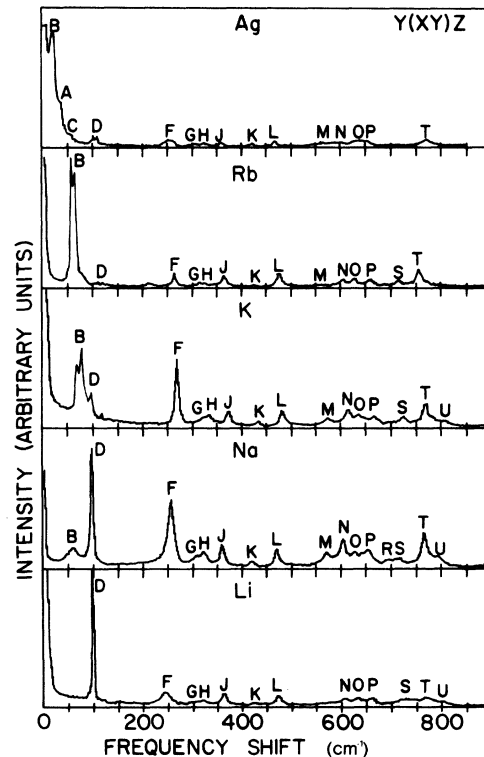


FIG. 2.  $Y(XY)Z$  spectra of  $\beta\text{-Al}_2\text{O}_3$  isomorphs obtained at  $300^\circ\text{K}$  for Rb, K, Na, and Li, and at  $77^\circ\text{K}$  for Ag.

The corresponding frequencies (in  $\text{cm}^{-1}$ ) are also summarized in Table I. Note that the data for Ag in the figures and tables were collected at 77°K. As can be seen from the table and the figures, the ZX spectra of all samples are quite similar and could be associated with the vibrations of the host lattice. The most obvious difference is that in Ag  $\beta$ -alumina there is a line at about  $60 \text{ cm}^{-1}$  which does not appear in any other samples. This might possibly be the vibration of  $\text{Ag}^+$  along the  $c$  direction ( $B_{2g}$  mode) if the symmetry of the crystal is slightly broken by disorder. The most interesting behavior actually occurs in the XX and XY polarizations ( $E_{2g}$  mode). The internal vibrations of the spinel blocks could account for the lines that are above  $250 \text{ cm}^{-1}$ , which are of unknown origin.

The ion dependent behavior occurs mostly in the region under  $250 \text{ cm}^{-1}$  in the XX and XY polarizations ( $E_{2g}$ ). In Table II, we list the frequencies associated with the vibrations of the cations. Note that nothing is listed for Li. This is because this line does not appear in the spectrum or it was covered by a line at about  $100 \text{ cm}^{-1}$ . The results for  $\text{Ag}^+$  and  $\text{Na}^+$  in  $\beta$ -alumina were discussed in

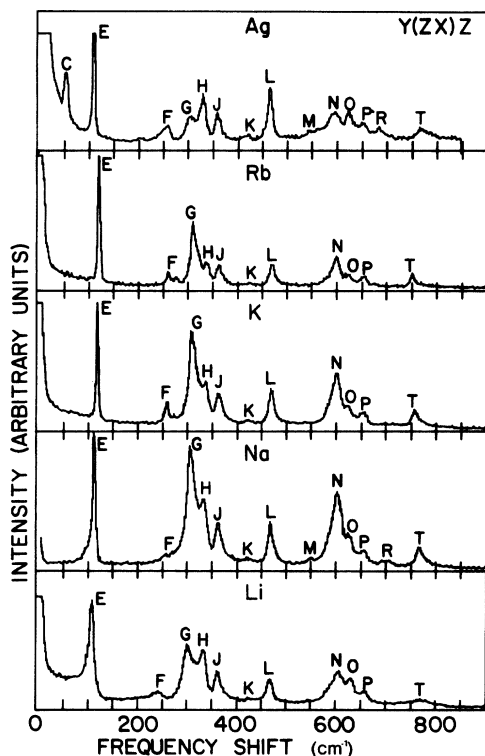


FIG. 3.  $Y(ZX)Z$  spectra of  $\beta\text{-Al}_2\text{O}_3$  isomorphs obtained at 300°K for Rb, K, Na, and Li, and at 77°K for Ag.

TABLE I. Observed frequencies of the Raman scattering spectra of  $\text{Li}^+$ ,  $\text{Na}^+$ ,  $\text{K}^+$ ,  $\text{Rb}^+$ , and  $\text{Ag}^+$  in  $\beta$ -alumina.

|                 | A  | B      | C  | D        | E   | F   | G   | H   | J   | K   | L   | M   | N   | O   | P   | R   | S   | T   | U   | V   | W   |
|-----------------|----|--------|----|----------|-----|-----|-----|-----|-----|-----|-----|-----|-----|-----|-----|-----|-----|-----|-----|-----|-----|
| Li              |    |        |    | 100      |     | 248 |     | 325 | 364 | 428 | 476 | 579 | 610 | 650 |     | 701 |     | 772 | 804 |     | 906 |
| Na              |    | 62     |    | 100      |     | 262 |     | 310 | 363 | 422 | 472 | 573 | 610 | 649 | 657 | 696 | 715 | 759 | 799 | 891 | 916 |
| K               |    | 72, 82 |    | 98       |     | 263 |     | 306 | 327 | 365 | 427 | 476 | 566 | 606 | 640 | 656 | 697 | 715 | 760 | 796 | 886 |
| Rb              |    | 63, 69 |    | 99       |     | 270 |     | 302 | 327 | 365 | 428 | 476 | 569 | 604 | 637 | 657 | 697 | 714 | 756 | 799 | 883 |
| Ag <sup>a</sup> | 38 | 29     | 64 | 107, 115 |     | 255 |     | 304 | 327 | 368 | 427 | 474 | 568 | 604 | 644 | 661 | 694 | 721 | 777 | 793 | 888 |
| Li              |    |        |    | 98       |     | 244 |     | 304 | 323 | 365 | 429 | 475 | 609 | 634 | 663 |     | 734 | 772 | 801 |     |     |
| Na              |    | 62     |    | 102      |     | 259 |     | 312 | 325 | 362 | 422 | 474 | 572 | 606 | 630 | 655 | 695 | 714 | 756 | 795 | 888 |
| K               |    | 73, 81 |    | 100      |     | 273 |     | 329 | 337 | 376 | 437 | 486 | 557 | 617 | 639 | 670 | 728 | 773 | 810 | 886 | 910 |
| Rb              |    | 64, 69 |    | 119      |     | 267 |     | 319 | 329 | 368 | 433 | 479 | 562 | 607 | 632 | 664 | 720 | 761 |     |     |     |
| Ag <sup>a</sup> | 38 | 29     | 67 | 107, 114 |     | 258 |     | 307 | 328 | 364 | 427 | 474 | 568 | 606 | 647 | 659 |     | 777 |     | 892 | 916 |
| Li              |    |        |    | 109      | 244 |     | 304 | 336 | 364 | 426 | 470 | 555 | 609 | 632 | 661 |     |     | 772 |     |     |     |
| Na              |    |        |    | 116      | 259 |     | 309 | 335 | 365 | 425 | 472 | 555 | 607 | 629 | 657 | 707 |     | 769 |     |     |     |
| K               |    |        |    | 123      | 261 |     | 315 | 341 | 366 | 425 | 476 | 555 | 607 | 625 | 657 |     |     | 760 |     |     |     |
| Rb              |    |        |    | 125      | 264 |     | 315 | 342 | 367 | 429 | 476 | 555 | 607 | 629 | 661 |     |     | 755 |     |     |     |
| Ag <sup>a</sup> |    |        | 59 | 118      | 262 |     | 309 | 334 | 362 | 427 | 471 | 559 | 603 | 630 | 657 | 692 |     | 772 |     |     |     |

<sup>a</sup> Data were collected at 77°K.

TABLE II. Frequencies associated with the vibrations of the cations.

| Ion             | $\omega_0^{13}$<br>( $\text{cm}^{-1}$ ) | $\frac{e^2 f(\epsilon)}{M}$ ( $\text{cm}^{-2}$ ) | Theory                             |                                    | Experiment                         |                                    |
|-----------------|---|--|------------------------------------|------------------------------------|------------------------------------|------------------------------------|
|                 |   |  | $\omega_r$<br>( $\text{cm}^{-1}$ ) | $\omega_s$<br>( $\text{cm}^{-1}$ ) | $\omega_r$<br>( $\text{cm}^{-1}$ ) | $\omega_i$<br>( $\text{cm}^{-1}$ ) |
| Na <sup>+</sup> | 90                                      | -5300  | 53                                 | 96                                 | 62                                 | 56                                 |
| K <sup>+</sup>  | 98                                      | -3126  | 80                                 | 101                                | 72, 82                             | 80                                 |
| Rb <sup>+</sup> | 78                                      | -1426  | 68                                 | 80                                 | 63, 69                             | 85                                 |
| Ag <sup>+</sup> | 42                                      | -1129  | 25                                 | 45                                 | 29                                 | 28                                 |

our previous paper.<sup>1</sup> In that paper, we showed that the lines at low frequencies for Ag<sup>+</sup> and Na<sup>+</sup> could be fitted by a simple Lorentzian response  $I \propto \omega(N+1)/[(\omega^2 - \omega_0^2)^2 + \gamma^2\omega^2]$ , with  $\omega_0$  and  $\gamma$  depending on the cation but not significantly on temperature. This still holds true for K<sup>+</sup> and Rb<sup>+</sup> in  $\beta$ -alumina. Another point that is obvious from the figures is that there are splittings in these lines for Ag<sup>+</sup> at low temperature (77 °K), and for K<sup>+</sup> and Rb<sup>+</sup> at room temperature. It is possible that these splittings result from either the in plane vibrational motion ( $E_{2g}$  mode) of the oxygens in the mirror planes, or from the vibrations of the cations in the inequivalent sites in the mirror plane.

At high temperatures in Ag  $\beta$ -Al<sub>2</sub>O<sub>3</sub>, intense inelastic scattering is observed at small frequency shifts. This feature becomes observable above about 600 °K, and increases in width with further increase in temperature. We attribute this behavior to the modulation of the Rayleigh scattering by the intersite hopping of the mobile cations. Typical data for Ag  $\beta$ -Al<sub>2</sub>O<sub>3</sub> are shown for Fig. 4. It is clear from a comparison of the data at 775 K and at 300 °K that additional scattered intensity has developed in the region below 10  $\text{cm}^{-1}$  at 775 °K. With the limited resolution of a double monochromator it is not possible to determine the exact shape of this low-frequency wing. However, light scattering from hopping, or relaxation, modes<sup>20</sup> is expected to have a Lorentzian shape with a width equal to the hopping rate of the mobile ions. Using an attempt frequency  $\omega_0 \cong 29 \text{ cm}^{-1}$  and an activation energy  $U \sim 0.18 \text{ eV}$  appropriate to Ag  $\beta$ -Al<sub>2</sub>O<sub>3</sub>, we estimate widths of  $\sim 0.05 \text{ cm}^{-1}$  at 300 °K and  $\sim 2.5 \text{ cm}^{-1}$  at 775 °K. These estimates are roughly consistent with the appearance of the observed low-frequency feature well above 300 °K. The reason for the failure to observe such a low-frequency wing for Na  $\beta$ -Al<sub>2</sub>O<sub>3</sub> is the very weak scattering produced by sodium ion displacements. This is probably related to much lower polarizability of the Na<sup>+</sup> ion compared with Ag<sup>+</sup>. In fact, we have found that the intensity of the cation  $E_{2g}$  vibration scales roughly as the square of the polarizability.

#### IV. THEORY

##### A. Stoichiometric structure

First the theory will be discussed for stoichiometric  $\beta$ -alumina. Here there is no excess of cation in the conducting plane. One cation is in each BR site, and the other sites are empty. There would be no superlattice. The effects of the excess cations, and the superlattice, will then be treated subsequently.

In either the infrared or Raman experiments, the optical field causes the Na or its substitutional

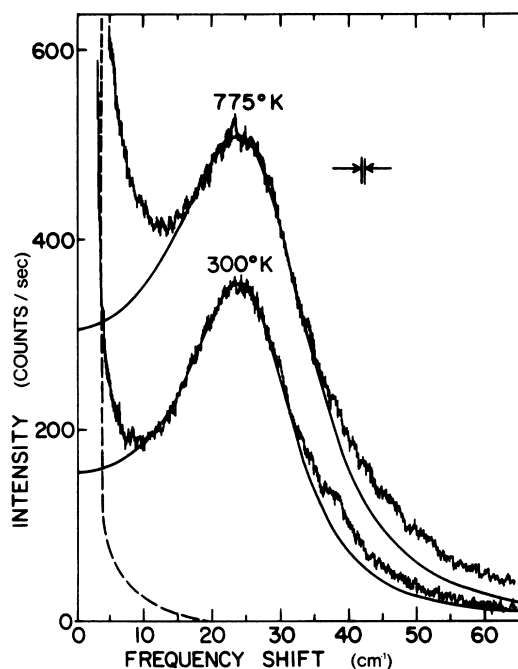


FIG. 4. Low-frequency  $Y(XY)Z$  spectra of Ag  $\beta$ -Al<sub>2</sub>O<sub>3</sub> at 300 °K and 775 °K. The vertical scale is appropriate to the 775 °K data; the 300 °K data would be 15% lower in intensity on that scale. The smooth, solid curves are Lorentzian fits to the data. The dashed curve shows the instrumental response to unshifted laser light of the same intensity as the Rayleigh peak in the 775 °K data.

cations to oscillate in space. The oscillating dipoles interact with each other by Coulomb forces. In a multipole expansion, the leading term, which is proportional to the oscillatory displacement of the ion, is the dipole-dipole interaction. When there are two ions—or dipoles—per unit cell, there are two distinct modes with separate eigenfrequencies. The difference between these frequencies is called the Davydov splitting.<sup>21,22</sup> There are many examples of these splittings in organic and inorganic solids.<sup>21-24</sup> Call the two frequencies  $\omega_i$  and  $\omega_r$ . They are given by the formulas

$$\begin{aligned}\omega_i^2 &= \omega_0^2 + (e^2/m)(t_{xx}^{(e)} + t_{xx}^{(i)}), \\ \omega_r^2 &= \omega_0^2 + (e^2/m)(t_{xx}^{(e)} - t_{xx}^{(i)}),\end{aligned}$$

where  $\omega_0$  is the frequency of a single cation oscillating by itself, and the other terms represent the dipolar coupling between cations. The first term in brackets represents the coupling between all atoms in the same plane. The second term is from the coupling between dipoles on adjacent planes. As we shall see, the coupling between more distant planes is negligible. In these summations we have assumed that all dipoles in a plane are in phase. This is essentially correct, since the two-dimensional sums converge over a distance much faster than the wavelength of light.

The frequency  $\omega_i$  represents the case where the dipoles in adjacent planes are in phase. This is the infrared active mode. The frequency  $\omega_r$  represents the case wherein the two vibrations in adjacent planes are out of phase. These are the Raman active modes in the case of the  $(x, y)$  vibrations.

The dipole coupling between two planes is small, and may be neglected. This may be shown using the standard formulas from plane-wise summation<sup>25,26</sup>

$$\begin{aligned}t_{xx}^{(i)} &= \sum_j \frac{1}{R_j^3} \left(1 - \frac{3R_{jx}^2}{R_j^2}\right) \\ &= \frac{2\pi}{A_0} \sum_G \frac{G_x^2}{G} e^{-\alpha C} \cos(\vec{\zeta}_0 \cdot \vec{G}), \\ R_j^2 &= C^2 + \vec{\zeta}_j^2,\end{aligned}$$

where  $\vec{G}$  are the two-dimensional reciprocal-lattice vectors of the plane, and  $A_0$  is the area of the unit cell. The vector  $\vec{\zeta}_j$  is the  $(x, y)$  part of the space vector  $\vec{R}_j$  between a cation in one plane, and the cations of the adjacent plane. And  $\vec{\zeta}_0$  is any one of these. In the ideal structure, there is a cation in each BR site. This structure forms a triangular lattice, with a basic reciprocal vector of magnitude  $G_0 = 4\pi/\alpha\sqrt{3}$ . Using  $c/\alpha$

$= 11.2/5.6 = 2.0$ , the exponential is  $e^{-14.5} = 10^{-6}$ . This is very small; thus,  $t^{(i)} = 0$ .

Thus we have shown that, to a high degree of accuracy, the Raman frequencies should equal those of infrared  $\omega_i = \omega_r$ . This occurrence is rather unusual. The conclusion only applies to the sodium vibrations in the plane or those of its substitutional cation.

The term  $t^{(e)}$  is the dipole coupling between a cation and all others in the same plane. A different set of formulas is used to evaluate it.<sup>26,27</sup> We obtain

$$t_{xx}^{(e)} = -5.517/a^3,$$

where  $a = 5.594 \text{ \AA}$ . For sodium this gives  $e^2 t^{(e)}/M = -5300 \text{ cm}^{-2}$ . This is a rather small dipole coupling term, compared to those typically found in exciton splittings, or other types of oscillations. But here it has a large effect, since  $\omega_0^2$  is unusually small. Thus the dipolar coupling between cations in the same plane provides a significant shift in the observed frequencies.

The frequencies  $\omega_0$  have been conveniently calculated by Wang, Gaffari, and Choi.<sup>19</sup> This is the vibrational frequency of one cation in a BR site, while all other ions are held fixed. Their results are shown in Table II for the four ions. The second column shows the dipole contribution, which differs for each ion according to its mass. The theoretical result obtained from

$$\omega_r = (\omega_0^2 + e^2 t^{(e)}/M)^{1/2}$$

is the third column. These compare favorably with the Raman and infrared experimental results.

The agreement between theory and experiment is very good. This success should be treated with caution. Two significant approximations have been made in the theory. This makes the good agreement with experiment surprising. The first approximation was made by Wang *et al.*<sup>19</sup> They fixed all ions but the one oscillating cation. One would expect some relaxation and coupling to the local neighbors of oxygen. The neglect of these effects is probably serious. The second approximation is our neglect of local field corrections in calculating the dipole interactions. This is very difficult to find in this heterogeneous material. In cubic crystals these effects are not large, since they enter as the factor<sup>27</sup>  $(1/\epsilon_0)[\frac{1}{3}(\epsilon_0 + 2)]^2$  which is near unity for most  $\epsilon_0$ . But  $\beta$ -alumina is far from cubic, and the actual local field corrections could be large. They were included by Wang *et al.* in their calculations.

Nevertheless, even if the theory is only regarded as approximate, the agreement with experiment permits one to draw some conclusions. First,

our assignment of these vibrations to one cation in the BR site appears reasonable. Both the frequency, the polarization rules, are in agreement with this assignment. According to the calculations of Wang *et al.*, much lower frequencies are obtained for the vibrations of two coupled ions in one cell. These are not observed in our experiment. In the model of nonstoichiometry proposed in Refs. 19 and 8, about (25–30)% of the cells are doubly occupied. Thus their vibrations should be easily observable in our experiment.

Our spectra show a splitting of this vibration for the three heaviest ions: K, Rb, and Ag. One could explain this second component as due to the doubly occupied cells. There are several difficulties with this proposal. First, this raises the question why Na lacks such a split-off component. Second, the splittings are observed to be small, while the theory suggests they are large. Thirdly, this requires the low-frequency component to have about 25% of the intensity of the other, while this is not the case; e.g., in Rb it is even stronger.

Another conclusion is that the frequencies do not scale as the inverse square root of the ion mass. Thus K and Rb have larger frequencies than Na, even with a larger mass. This is explained in terms of their larger size, and commensurate stronger coupling to the neighboring oxygens.<sup>19</sup>

### B. Superlattice in Ag $\beta$ -alumina

LeCars *et al.*<sup>6</sup> reported a superlattice at low temperature. This structure is shown in Fig. (5a). The superlattice contains three normal unit cells on a mirror plane, and contains four Ag ions: three in BR sites, and one in a anti-BR site. The Ag ions in anti-BR sites form a superlattice which is a triangular lattice with lattice constant  $\sqrt{3}a$ . Two groups have reported directly conflicting results on how this superlattice changes with temperature.<sup>6,8,28</sup>

We shall still neglect the coupling between ions in different planes. Thus we need to find the normal modes of the superlattice in a single mirror plane. The  $(x, y)$  vibrations of the three Ag ions in BR sites yield six possible normal modes. In  $D_{6h}$  symmetry, these modes are  $A_{1g}$ ,  $A_{2g}$  and two pairs are  $E_{2g}$ . A crystal-field analysis shows that one pair of  $E_{2g}$  modes are the same as discussed above in A: the modes where all ions vibrate in phase in the same direction. The other pair of  $E_{2g}$  modes have the three Ag ions, in BR sites in the superlattice cell, vibrating such that the center of mass is fixed. Thus these modes

would not be ir active, but only Raman active. A crystal-field calculation among the interacting vibrations of the Ag ions in BR sites show that the collective vibrational frequency is  $\omega_s$ ,

$$\omega_s^2 = \omega_0^2 + (e^2/M)t^{(a)},$$

where we obtain for

$$t^{(a)} = 1.166/a^3.$$

Thus this new Raman-active mode, which is introduced by the superlattice, is at a higher frequency than  $\omega_0$ . Our calculated value for  $\omega_s$  is shown in Table II.

Our hypothesis is that the splitting in the low-frequency  $E_{2g}$  peak is caused by the superlattice. One peak is  $\omega_r$  and the other is  $\omega_s$ . In order for this explanation to be tenable, several modifications of the theory are necessary. First,  $\omega_0$  must be much smaller than given in Ref. 19, and should be nearer to 20–25  $\text{cm}^{-1}$  for Ag. Second, the crystal-field splittings should be much

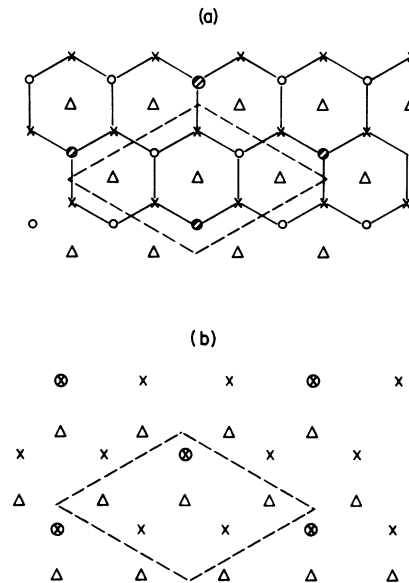


FIG. 5. (a) Superlattice of Ag  $\beta$ -alumina. The  $\times$  are Beavers-Ross (BR) sites, which are all occupied, and the  $\Delta$  are in-plane oxygen sites. The small shaded circles are empty anti-BR sites, and the large shaded circles are occupied anti-BR sites. The unit cell of the superlattice is shown dashed. It contains four Ag ions, and its area is three times that of the usual lattice cell. (b) Superlattice of K  $\beta$ -alumina. The  $\times$  are singly occupied BR sites, and the  $\otimes$  are BR sites with two K ions. The  $\Delta$  are in-plane oxygen sites. The superlattice is now of the double occupied BR sites. In these sites, the two K ions actually sit in positions midway between the oxygens. Again there are four ions per unit cell of the superlattice.

smaller than we calculate—perhaps the reduction is caused by local field effects. Our hypothesis must remain tentative until these theoretical points are tested further. But the virtue of this hypothesis is that it explains why the splittings are observed at all.

The  $A_{2g}$  mode is Raman inactive, but the  $A_{1g}$  mode should be observed in  $(XX)$  and  $(ZZ)$  polarization. It does not seem to appear—i.e., there are no modes which appear in  $(XX)$  but not in  $(XY)$  in Figs. 1 and 2.

An examination of the  $(z)$  vibrations of the ions shows a new Raman-active mode in the superlattice, which was absent in the ordinary lattice. The three Ag ions in BR sites oscillate in a mode which would be observable in  $(ZX)$  geometry. This is tentatively identified as the anomalous peak  $C$  in Fig. 3(a) at  $59\text{ cm}^{-1}$ . It does not appear to change intensity much between  $4^\circ\text{K}$  and room temperature.

### C. Superlattice in Na, K, Rb $\beta$ -alumina

A superlattice was also reported for these materials.<sup>28</sup> Again there are four cations in a superlattice cell which is three times the area of a usual cell. This structure is shown in Fig. 5(b). Now there are two cations in BR sites, and another two which doubly occupy the remaining cell—each in a bridge site. The superlattice is of the doubly occupied cells. Obviously the group theory is different than for the Ag superlattice: there are two cations in BR sites instead of three. The  $(x, y)$  motions of these two cations yield two pairs of  $E$  modes which are Raman active. One pair of  $E$  modes has the two cations oscillating in phase, and are described by the same formula for  $\omega_r$ . The other pair of  $E$  modes has them exactly out of phase, and is again described by the equation for  $\omega_s$ . These values are shown in Table II.

For K and Rb the predicted splittings are again about a factor of 2 too large. No experimental splitting is observed for Na, although it too is reported to have a superlattice. This is a definite contradiction to the hypothesis that the splittings are due to the superlattice. Although we regard our hypothesis as reasonable, it must remain unsettled until the question is answered regarding the sodium splittings or superlattice. We do note that the report of the sodium superlattice was confusing, in that the x-ray patterns were said to be like Ag rather than K, although Na does not like to occupy anti-BR sites. We have already remarked about another unanswered question regarding the present results and the superlattice—why do not we, nor the ir, see the vibrations of ions in the doubly occupied cells?

## V. DISCUSSION

We also observe that the low-frequency lines of  $\text{Na}^+$ ,  $\text{Ag}^+$ ,  $\text{K}^+$ , and  $\text{Rb}^+$  in  $\beta$ -alumina do not change significantly with the temperature. As mentioned in our previous paper,  $\omega_0, \gamma$  changed by only a few  $\text{cm}^{-1}$  from room temperature to about  $800^\circ\text{K}$ . This clearly does not agree with the assumption of Huberman and Sen<sup>13</sup> of the existence of a cutoff frequency  $\omega_0$  which is temperature dependent.

Several of the Raman-active modes observed in the region of  $100\text{ cm}^{-1}$  and below appear to correspond to vibrations observed by neutron scattering.<sup>9</sup> A weak line is observed at  $\sim 300^\circ\text{K}$  in  $XX$  geometry in the Ag and Rb isomorphs at about  $38\text{ cm}^{-1}$ . This feature appears clearly in the  $300^\circ\text{K}$  Ag data in Fig. 4. A similar line is observed in the  $XX$  spectrum of Na  $\beta$ - $\text{Al}_2\text{O}_3$  at  $77^\circ\text{K}$ . This vibration is possibly the zone-center shearing motion of the two spinel blocks, shown in Fig. 6(a) observed in neutron scattering at about  $5\text{ meV}$ .<sup>9</sup> Since this is an odd-parity vibration, it would appear only as a result of the disorder in the lattice. Two Raman-active vibrations are observed near  $100\text{ cm}^{-1}$ , one transforming as  $E_{2g}$  and the other as  $E_{1g}$ . The intensity of the  $E_{2g}$  mode is very strongly influenced by the size of the cation on the mirror plane sites. For Na and Ag this vibration is one of the strongest in the spectrum, while it is barely observable in Rb  $\beta$ - $\text{Al}_2\text{O}_3$ . For this reason, we speculate that this vibration involves the combined motions of the mirror-plane oxygens and cations as well as some shearing of the spinel blocks as shown schematically in Fig. 6(b). It is essentially one of the  $E_g$  modes associated with the combined displacements of the cations and oxygens mentioned in Sec. III. This vibration is very probably the transverse mode observed with neutron scattering<sup>9</sup> at  $12\text{ meV}$  ( $96\text{ cm}^{-1}$ ) in Na  $\beta$ - $\text{Al}_2\text{O}_3$ . The  $E_{1g}$  vi-

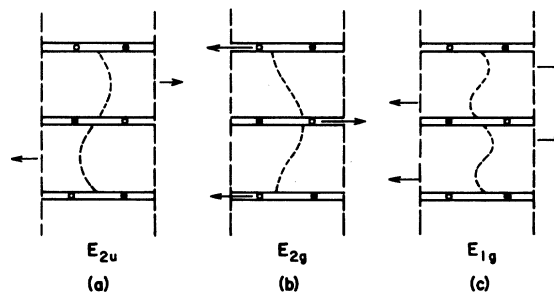


FIG. 6. Schematic illustration of the displacements of the spinel blocks, and ions in the mirror plane, for three of the low-frequency vibrations observed in  $\beta$ - $\text{Al}_2\text{O}_3$  isomorphs. Open and closed circles represent oxygen ions and cations, respectively, in the mirror plane.

bration at  $114\text{ cm}^{-1}$  in the Na isomorph is assigned to a spinel-block shear of the type shown in Fig. 6(c). This assignment is based on the low frequency of the mode, which suggests that it is a bulk distortion of the spinel blocks, and the fact that the mode in Fig. 6(c) is the only lowest-frequency  $E_{1g}$  mode of that type. A phonon branch has been observed in neutron scattering<sup>9</sup> which is at  $14.3\text{ meV}$  ( $114\text{ cm}^{-1}$ ); however, that phonon branch is identified as being longitudinal, which is not in agreement with the  $E_{1g}$  character of the Raman-active mode of the same frequency.

We would also like to point out that the largest departures from the  $D_{6h}$  polarization selection rules occur for the higher-frequency vibrations

associated with internal modes of the spinel blocks. This is consistent with the large concentration of Frenkel defects reported in the spinel blocks.<sup>15</sup> In contrast, the selection rules for the low-frequency vibrations of the mobile cations are well obeyed, despite the extensive disorder which is thought to exist in the conducting planes.

Finally, there are presently two conflicting results on how the superlattice in Ag  $\beta$ -alumina changes with temperature. An investigation of the splittings of the  $B$  and  $D$  lines in Ag  $\beta$ -alumina as a function of temperature is being conducted in order to gain some insight to the above problem. Also a study of the "relaxation mode" will be pursued further.

\*Research supported by the NSF.

†Present address: Clarendon Laboratory, Oxford, England OX1 3PU.

<sup>1</sup>L. L. Chase, C. H. Hao, and G. D. Mahan, *Solid State Commun.* **18**, 401 (1976).

<sup>2</sup>D. Jerome and J. P. Boilot, *J. Phys. Lett.* **35**, L129 (1974); I. Chung, H. Story, and W. L. Roth, *Bull. Am. Phys. Soc.* **19**, 202 (1974).

<sup>3</sup>J. T. Kummer, *Prog. Solid State Chem.* **7**, 141 (1972).

<sup>4</sup>Y. Y. Yao and J. T. Kummer, *J. Inorg. Nucl. Chem.* **29**, 2453 (1967).

<sup>5</sup>S. J. Allen, Jr. and J. P. Remeika, *Phys. Rev. Lett.* **33**, 1478 (1974).

<sup>6</sup>Y. LeCars, R. Comes, L. Deschamps, and J. Thery, *Acta Crystallogr. A* **30**, 305 (1974).

<sup>7</sup>J. P. Bailot, J. Thery, R. Collongues, R. Comes, A. Guiner *Acta Crystallogr.* (to be published).

<sup>8</sup>D. B. McWhan, S. J. Allen, Jr., J. P. Remeika, and P. D. Dernier, *Phys. Rev. Lett.* **35**, 953 (1975).

<sup>9</sup>D. B. McWhan, S. Shapiro, J. P. Remeika, G. Shirane *J. Phys. C* **8**, L487 (1975).

<sup>10</sup>M. J. Rice and W. L. Roth, *J. Solid State Chem.* **4**, 294 (1972).

<sup>11</sup>H. Sato and R. Kikuchi, *J. Chem. Phys.* **55**, 677 (1971).

<sup>12</sup>W. Van Gool and P. H. Bottelberghs, *J. Solid State Chem.* **7**, 59 (1973).

<sup>13</sup>B. A. Huberman and P. N. Sen, *Phys. Rev. Lett.* **33**, 1379 (1974).

<sup>14</sup>W. L. Roth, *J. Solid State Chem.* **4**, 60 (1972).

<sup>15</sup>W. L. Roth, General Electric Technical Information Series report No. 74 CRD 054 (unpublished).

<sup>16</sup>U. Strom, P. C. Taylor, S. G. Bishop, T. L. Reinecke, K. L. Ngai (to be published).

<sup>17</sup>A. S. Barker, Jr., *Phys. Rev.* **132**, 1474 (1963).

<sup>18</sup>S. P. S. Porto and R. S. Krishnam, *J. Chem. Phys.* **47**, 1009 (1967).

<sup>19</sup>J. C. Wang, M. Gaffari, and S. Choi, *J. Chem. Phys.* **63**, 772 (1975).

<sup>20</sup>M. V. Klein, Third International Conference on Light Scattering in Solids, Campinas, Brazil, July, 1975 (unpublished).

<sup>21</sup>A. S. Davydaov, *Theory of Molecular Excitons* (McGraw-Hill, New York, 1962).

<sup>22</sup>G. D. Mahan, in *Electronic Structure of Polymers and Molecular Crystals*, edited by J. Andre and J. Ladik (Plenum, New York, 1975).

<sup>23</sup>L. C. Kravitz, J. D. Kingsley, and E. L. Elkin, *J. Chem. Phys.* **49**, 4600 (1968).

<sup>24</sup>J. D. Kingsley, G. D. Mahan, and L. C. Kravitz, *J. Chem. Phys.* **49**, 4610 (1968).

<sup>25</sup>G. D. Mahan and G. Obermair, *Phys. Rev.* **183**, 834 (1969).

<sup>26</sup>B. R. A. Nijboer and F. W. deWette, *Physica (Utr.)* **24**, 422 (1958).

<sup>27</sup>G. D. Mahan, *Phys. Rev.* **153**, 983 (1967).

<sup>28</sup>Values of correlation lengths in Ref. 8 were corrected recently.